MORPHOLOGICAL ENGINEERING OF PLASMONIC NANOSTRUCTURES: SIMULATION OF OPTICAL RESPONSE FOR NANOPARTICLES WITH BASIC GEOMETRIES

T. BULAVINETS, V. GROKHOTOV, I. HELZHYNSKYY, B. BULAVINETS, P. STAKHIRA*, I. YAREMCHUK

Lviv Polytechnic National University, Stepana Bandery Str., 12, 79000, Lviv, Ukraine *Corresponding author: pavlo.y.stakhira@lpnu.ua

Received: 20.10.2025

Abstract. A systematic numerical study of the plasmonic properties of metal nanoparticles with basic geometries (ellipsoidal, cubic, cylindrical, and prismatic) was conducted using the discrete dipole approximation. It has been demonstrated that the optical response of all anisotropic nanoparticles is critically dependent on spatial orientation. The positions of plasmon resonances can be tuned over a wide wavelength range by varying geometric parameters. The universal physical mechanisms that determine plasmonic behavior have been identified. These include the dependence of resonance on the depolarization factor, field localization in regions of maximum curvature, multimodal resonances for complex geometries, and size-dependent radiative damping. These results provide the scientific background for the morphological engineering of plasmonic nanostructures with optimized characteristics for use in optoelectronic, sensor, and spectroscopic applications.

Keywords: localized surface plasmon resonance, nanoparticles, discrete dipole method, electric field localization

UDC: 621.38.049.77; 621.375.82.01

DOI: 10.3116/16091833/Ukr.J.Phys.Opt.2026.01054

This work is licensed under the Creative Commons Attribution International License (CC BY 4.0).

1. Introduction

Plasmonic nanoparticles are a key element of modern nanophotonics. They provide strong localization and amplification of the electromagnetic field when light interacts with free electrons in metals, a phenomenon known as localized surface plasmon resonance (LSPR). This physical phenomenon is the collective oscillation of free electrons at the metal-dielectric interface, excited by electromagnetic radiation [1]. It provides significant enhancement of the local electromagnetic field, as well as anomalously high cross sections for light scattering and absorption [2,3]. These properties make plasmonic nanostructures highly desirable for use in sensing [4-6], surface-enhanced Raman spectroscopy (SERS) [7-9], photovoltaics [10-12], biomedicine [13,14], and organic electronics [15-18].

Plasmonic nanoparticles exhibit strong near-field enhancement. This depends on the environment and neighboring particles [19]. This requires accurate calculation of electromagnetic coupling in nanoparticle assemblies, accounting for hot spots where fields can be several times stronger. The influence of substrates and the environment adds to the complexity [20]. It is worth noting that plasmonic nanoparticles are highly sensitive to the polarization of incident light. This property is particularly apparent in particles of complex shapes or assemblies of nanoparticles. Take nanorods, for instance. Altering the polarization can entirely transform the absorption or scattering spectrum [21]. Accurately predicting the effects of polarization requires

three-dimensional modelling of nanoparticle shape, consideration of particle interactions in assemblies, and calculation of local fields for different directions of the electric vector.

The geometry of nanoparticles is crucial in determining their optical properties. Ellipsoidal nanoparticles can enhance the efficiency of sensors based on surface plasmon resonance due to their polarization-dependent absorption properties [22]. Alternatively, they can be used in solar cell structures to increase photocurrent, thereby reducing the thickness of the active layer and the device's toxicity [23]. Cubic nanoparticles are used in plasmonic sensors because they can create intense electric fields at their sharp corners [24]. Their shape and large surface area give them high catalytic activity [25]. Due to their optical properties and their ability to efficiently transmit light at the nano- and microscales, cylindrical nanoparticles offer significant advantages in real-world devices. Applications include plasmonic waveguides, solar cells, and novel optical materials [26, 27]. The anisotropic shape of prism-shaped nanoparticles gives them unique optical properties. These properties can be used to create highly sensitive sensors capable of detecting low concentrations of molecules in solar cells, significantly improving their efficiency [28, 29].

The shape, size, and aspect ratio of particles directly affect the spectral position of the plasmon resonance, the width of the resonance band, and the spatial distribution of the electromagnetic field [30]. Even minor geometric deviations can alter the resonant frequency. Spherical nanoparticles are the simplest geometry and exhibit a single resonant peak. The position of this peak is determined by the material of the particle and the dielectric properties of the surrounding medium. Classical Mie theory provides an analytical solution to Maxwell's equations for such particles, enabling accurate calculations of scattering, absorption, and extinction cross sections [31]. At the same time, nanoparticles with more complex geometries, characterized by multiple resonant modes, require more advanced numerical methods. These include the finite-difference time-domain (FDTD) method [32], the finite element method (FEM) [33], and the discrete dipole approximation (DDA) [34]. The discrete dipole approximation (DDA) provides a flexible approach for studying how nanoparticles, regardless of form or composition, interact with light [35, 36]. The DDA method involves representing a nanoparticle as an array of point dipoles located at the nodes of a cubic lattice. Each dipole interacts with the external electromagnetic field and the fields created by the other dipoles. The polarization of the i-th dipole is determined by a self-consistent system of equations. Solving these equations allows us to calculate the full optical response of the system. This approach enables the optical properties of particles of arbitrary shape and composition to be calculated with high accuracy, overcoming the limitations inherent in analytical methods.

This study aims to provide a systematic, theoretical analysis of the optical properties of plasmonic nanoparticles of various geometries when placed in an organic matrix. In particular, extinction cross-section calculations were performed, and the spatial distribution of the electromagnetic field in the vicinity of the nanostructures during resonant excitation was obtained. This comprehensive approach enables us to establish relationships between nanoparticles' geometric parameters and their optical properties. This is of great importance for the rational design of plasmonic nanosystems with controlled properties. Using different forms of silver nanoparticles in organic light-emitting diodes allows their optical properties to be fine-tuned, thereby increasing the devices' efficiency and functionality. This opens new opportunities to develop light-emitting structures for use across various fields.

2. Methodology of research

The nanoparticles were made of silver, with tabulated values of the complex dielectric function. These nanoparticles exhibit pronounced plasmon resonances in the visible and near-infrared regions of the spectrum, making them promising candidates for optoelectronic devices. The refractive index of the dielectric matrix was set to 1.7 for the calculations, which corresponds to typical values for organic materials used in electron- and hole-transport layers of organic light-emitting diodes. A numerical simulation was performed using the Discrete Dipole Approximation (DDA) method, which is implemented in the DDSCAT+ software package - a cloud-based version of the DDSCAT 7.3 classic package. Geometric models were designed using professional three-dimensional modelling software, Blender. The created objects were converted into an array of electric dipoles within a single block. The DDA Convert tool, part of the DDSCAT+ software package ecosystem, was used to perform the conversion. In the DDA Convert settings space, the object shape was filled with dipoles at a resolution level of 'medium', and a 'dipole per nanometer' was selected to discretize the nanoparticles. The number of dipoles in each model was automatically determined during conversion to the DDSCAT+ geometry format, based on the object's actual dimensions. The optical parameters of the studied structures were then calculated using the electric dipoles represented by the number of points. In this study, the duration of one simulation did not exceed 12 hours. This depended primarily on the current load and the availability of the remote servers used by the DDSCAT+ platform. All nanoparticles were modelled with a maximum size of 80 nm to make sure that different shapes could be consistently compared. A set of three-dimensional geometric models of silver nanoparticles in four basic configurations has been developed: ellipsoidal, cubic, cylindrical and prismatic. A series of models with varying geometric parameters were created for each morphology. We parameterized ellipsoidal nanoparticles by the lengths of three semiaxes, which enabled us to investigate the effect of aspect ratio on the optical response. The precise representation of vertices and edges in space was of the utmost importance when defining cubic structures, with their edges measured in units of length. The height and diameter of cylindrical nanoparticles were characterized, allowing for independent variation of these parameters. Prismatic structures were modelled as square-based pyramids of varying heights. This allowed the sharpness of the apex to be controlled and enabled investigation of the effect of localizing an electric field at sharp edges.

To validate the accuracy of the calculations, we compared the results for spherical silver nanoparticles with a diameter of 20 nm located in a medium with a refractive index of 1.7 (Fig. 1). The dielectric constant of silver was obtained from the *mtable* file, which contains tabulated data from [37]. Dispersion or temperature corrections were not accounted for in the calculations. The extinction spectra were calculated using the DDA method implemented in DDSCAT and the dipole approximation. The deviation in the position of the plasmon resonance maximum was less than 2 nm, and the relative error in the extinction factor was less than 3% across the entire studied spectral range.

Using the DDSCAT+ platform gave us access to remote computing servers, enabling us to perform parallel calculations for a variety of geometric configurations and spectral ranges.

It is important to consider the limitations of the discrete dipole method when interpreting the results. Firstly, the method's accuracy may decrease for large particles

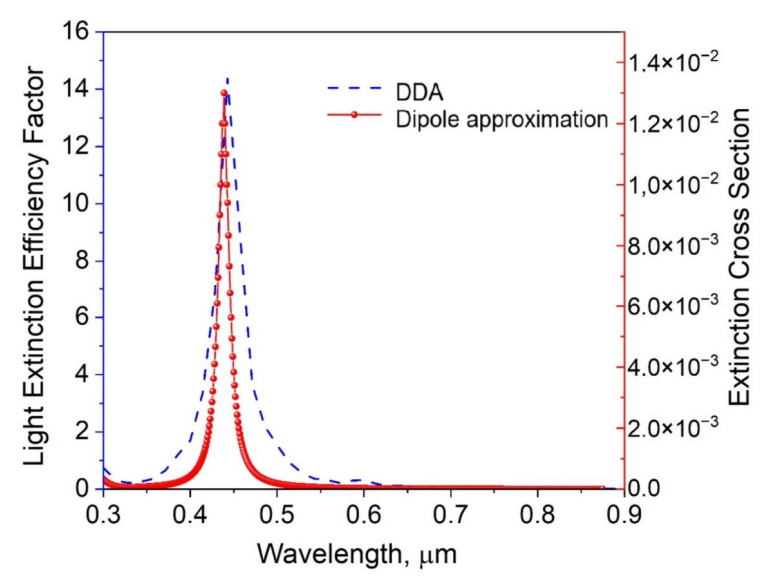


Fig. 1. The extinction spectrum of a spherical nanoparticle, calculated using the DDSCAT software environment and the dipole approximation method.

(those larger than 25 times the wavelength), especially for materials with a high refractive index [38]. In our study, the effective radii of all the considered nanoparticles ranged from 20 to 80 nm. This corresponds to size parameters of 5–20 in the spectral range of 400–800 nm, i.e., well within the method's applicability. Secondly, there are significant difficulties when modelling particles with sharp corners and edges. In such regions, the electric field changes abruptly over distances smaller than the sampling step. This leads to shape errors because the particle edges cross the sampling cells [39].

3. Results and discussion

A systematic study of the effect of the medium's refractive index revealed universal patterns across all morphologies. Increasing the refractive index of the surrounding medium from 1.0 to 1.7 shifts the extinction maximum towards the red end of the spectrum. This shift varies with nanoparticle geometry, ranging from 130 to 190 nm. At the same time, an increase in the extinction efficiency coefficient is observed. It indicates an increased interaction between the nanoparticle and electromagnetic radiation in a dielectric medium with a higher polarizability. This phenomenon is associated with a change in the conditions required to fulfil the Froelich resonance condition. The resonance condition is fulfilled at longer wavelengths when there is an increase in the dielectric constant of the medium. For ellipsoidal nanoparticles with an axis ratio of 2:1, changing the refractive index from 1.0 to 1.7 shifts the extinction maximum from 418 nm to 608 nm (Fig. 2b), i.e., by 190 nm. This shift is the largest observed among the studied geometries, reflecting the longitudinal plasmon mode's high sensitivity to the dielectric environment of the ellipsoids.

The spatial orientation of anisotropic nanoparticles relative to the direction of propagation and polarization of the incident wave significantly impacts their optical response through depolarization. This effect manifests as the depolarization factor depending on the nanoparticle geometry and the direction of the electric field oscillations. A change in orientation results in a cardinal transformation of the plasmonic properties of

ellipsoidal nanoparticles with an axis ratio of 2:1 (40×20 nm). In the *Y*-polarization configuration, the electric field is perpendicular to the long axis, and a transverse plasmon mode with an extinction maximum at 410 nm is excited. In *Z*-polarization, the field is parallel to the long axis, and a longitudinal mode is excited, with a maximum at 610 nm, resulting in a 200-nm shift (Fig. 2c).

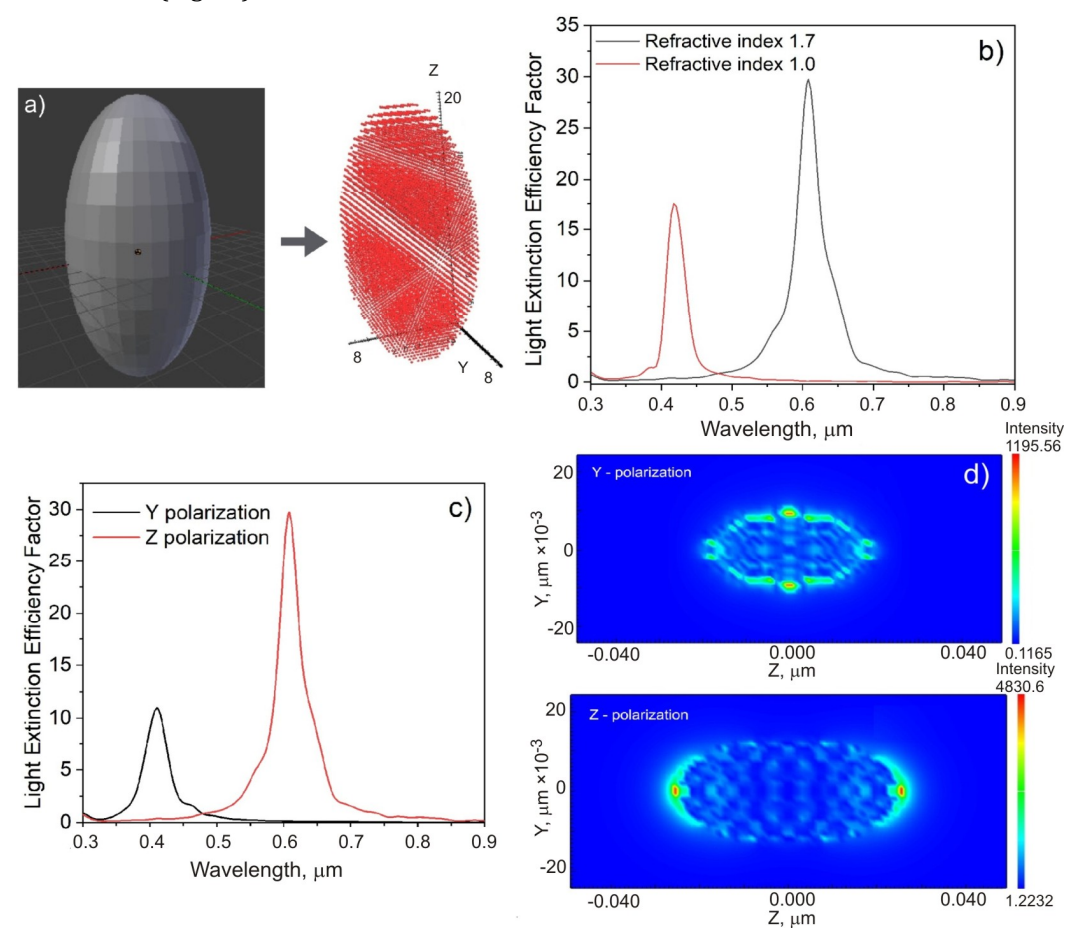


Fig. 2. Ellipsoidal nanoparticles: three-dimensional geometric model (a); dependence of the extinction coefficient on the wavelength for different refractive indices of the surrounding medium (b); dependence of the extinction coefficient on the wavelength for different directions of polarization (c); distribution of the electromagnetic field (d).

The difference in electric field localization is particularly striking: maximum intensity increases from 1.596 V/m with *Y*-polarization to 4.831 V/m with *Z*-polarization (i.e., three times as much) (Fig. 2d). The reason for this is the fundamental principle of field concentration in areas where the local curvature is at its greatest. In the case of longitudinal polarization, the electric field is concentrated at the rounded ends of the ellipsoid where the curvature is greatest. In contrast, with transverse polarization, the field is distributed across the entire nanoparticle surface.

The geometry of the ellipsoid provides the most predictable and consistent relationship between the plasmonic properties and the aspect ratio. A systematic study of ellipsoids with a constant diameter of 20 nm and varying lengths between 20 and 80 nm revealed a clear correlation between the geometric parameters and the spectral position of the resonance (Fig. 3). An increase in nanoparticle length is accompanied by a red shift in the extinction maximum of the

longitudinal plasmon mode, ranging from 444 nm for an ellipsoidal particle measuring 20×20 nm to 956 nm for a highly elongated ellipsoid measuring 20×80 nm. Thus, tuning the plasmon resonance across a wide spectral range from the visible to the near-infrared can be achieved by varying the aspect ratio from 1:1 to 4:1.

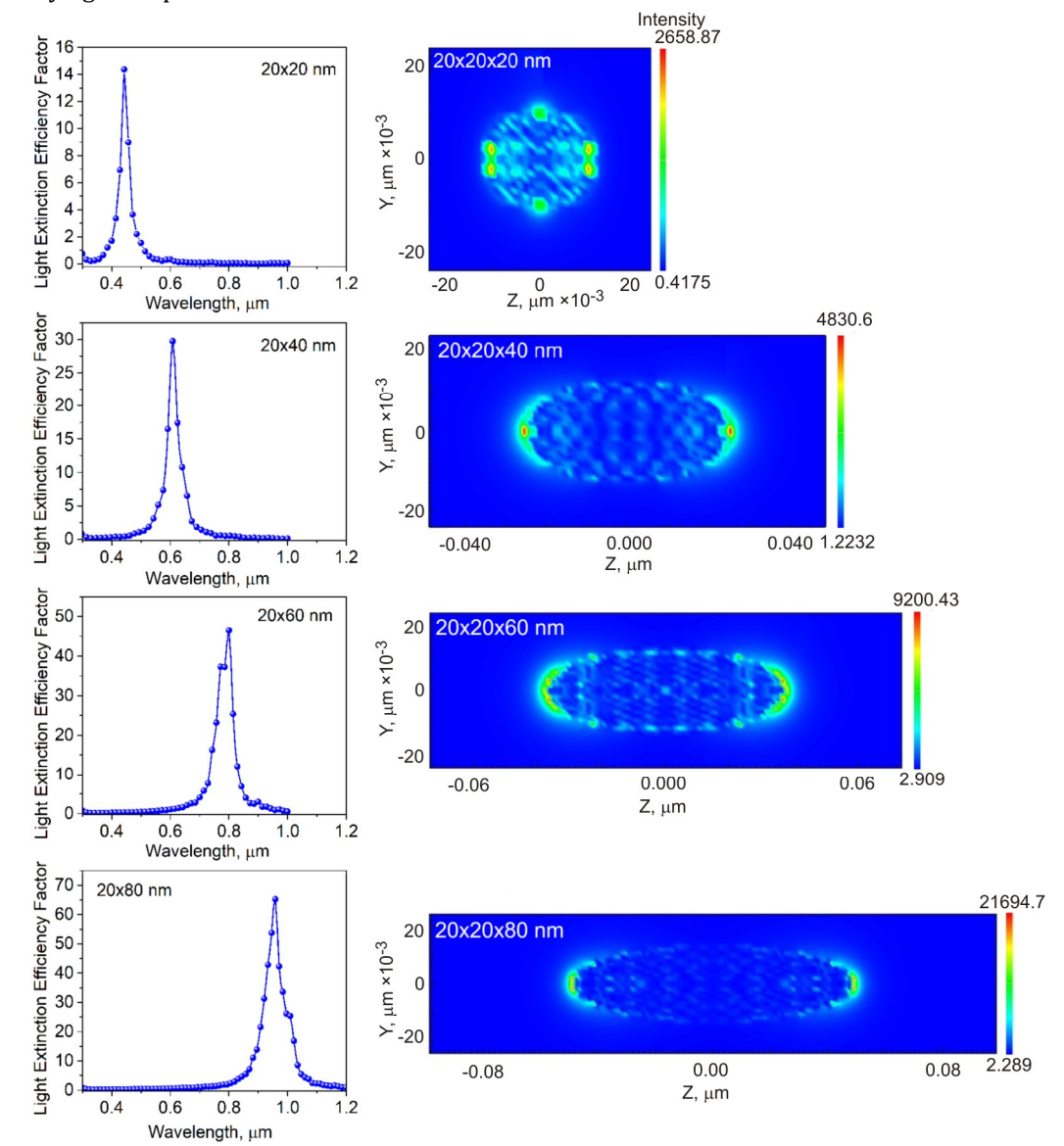


Fig. 3. Ellipsoidal nanoparticles: the dependence of the extinction coefficient on the wavelength and electromagnetic field distribution for different nanoparticle sizes.

At the same time, the extinction efficiency coefficient increases, indicating that plasmon interactions increase with the aspect ratio. This is due to the decrease in the depolarization factor for the longitudinal mode. The more elongated the particle, the weaker the internal depolarization field that counteracts the collective oscillations of electrons along the long axis becomes.

As the aspect ratio increases, a qualitative change in the spatial distribution of the electric field becomes apparent. For a particle measuring 20×20 nm, a nearly uniform field distribution is

observed across the surface, with maxima occurring at the poles in relation to the polarization direction of the incident wave. The field becomes localized at the rounded ends of the ellipsoid when it is elongated. The maximum field strength shows a non-monotonic dependence on the aspect ratio, peaking at intermediate geometries. This is due to competition between two physical mechanisms: field concentration in areas of high curvature, which increases with the aspect ratio, and radiative attenuation, which increases with particle size.

The observed patterns are physically based on the dependence of the resonance condition on the depolarization factor L. For ellipsoids, L is determined by the ratio of the axes and can be calculated analytically. The resonance condition can be expressed as $Re(\varepsilon(\omega)) = -\varepsilon_m \left(\frac{1}{L} - 1\right)$ [40], where $\varepsilon(\omega)$ is the dielectric function of the metal, ε_m is the

dielectric constant of the medium. A single resonance is the result of L=1/3 for all three spatial directions, for a spherical particle. The longitudinal depolarization factor decreases (L<1/3) for an elongated ellipsoid, while the transverse factors increase. This causes the splitting of the plasmon modes, with the longitudinal mode shifting to the red region and the transverse modes shifting to the blue region.

Cubic geometry represents a distinct class of plasmonic nanostructures characterized by complex multimodal behavior due to their high symmetry and the presence of structural elements with varying local curvatures. Cubic nanoparticles with an edge of 20 nm show not only a shift in resonances, but also a transformation of the spectral structure. Two peaks are observed in air at 375 and 400 nm. In a medium with a refractive index of 1.7, however, a complex multimodal structure emerges, with a dominant resonance at 558 nm and additional maxima at 467 and 499 nm (see Fig. 4b). Two more small maxima can also be identified. These are at approximately 350 and 400 nm. This splitting occurs due to the excitation of different plasmon modes, each with a different sensitivity to the dielectric environment. Analysis of the spatial distribution of electric fields relative to the polarization direction of the incident wave was not performed since regular cubes were considered, for which the polarization direction is irrelevant.

A study of silver nanocubes with edge sizes ranging from 20 to 80 nm revealed a complex evolution of their spectral characteristics. Unlike ellipsoids, for which a monotonic shift in a single dominant resonance is observed, cubes are characterized by a multimodal extinction spectrum structure that transforms with particle size (see Fig. 5). The excitation of

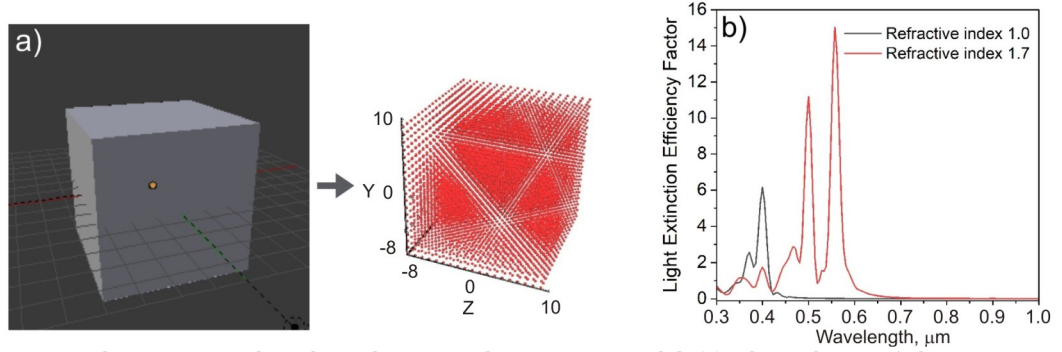


Fig. 4. Cubic nanoparticles: three-dimensional geometric model (a); dependence of the extinction coefficient on the wavelength for different refractive indices of the surrounding medium (b).

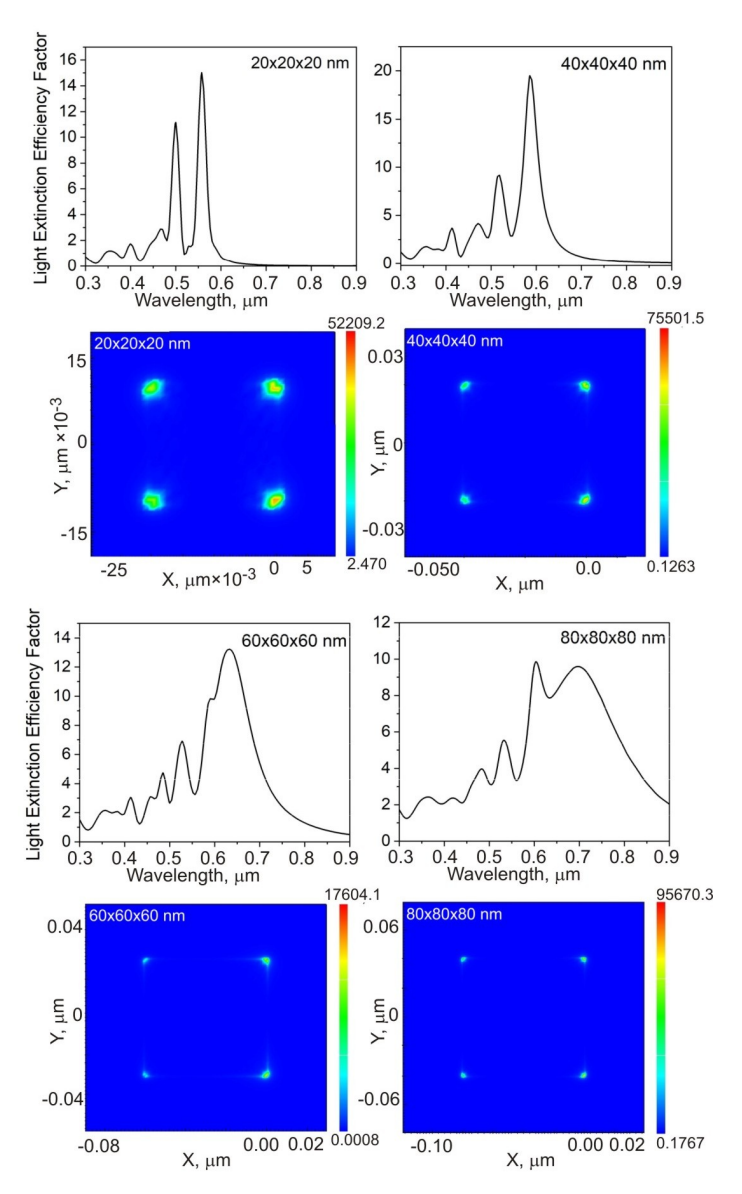


Fig. 5. Cubic nanoparticles: dependence of the extinction coefficient on the wavelength and electromagnetic field distribution for different sizes of the nanoparticles.

corner, edge, and face plasmon modes is caused by cubic symmetry. These plasmon modes have different spectral positions and size sensitivities [41]. The highest resonant frequency is exhibited by angular modes that are localized at the cube's vertices, where the curvature is at its peak. An intermediate spectral position is occupied by edge modes, while face modes resonate at the lowest frequencies. Not only does a general red shift of all spectral features occur when the cube edge increases from 20 to 80 nm, but there is also a change in the relative intensities of individual modes. This is due to size-dependent radiative attenuation. For larger particles, radiative losses become comparable to ohmic losses. This leads to the broadening of spectral peaks and changes in the amplitude ratio of different modes [42]. The electric field distribution around cubic nanoparticles invariably exhibits maximum localization at the cube's vertices, where the surface curvature is most significant (see Fig. 5).

This is consistent with the classical electrostatic principle that charge is concentrated on the sharp protrusions of a conductor, meaning that the surface charge density is proportional to the local curvature. The electric field strength at the vertices can exceed the average value at the faces by a factor of ten. This makes the vertices of cubic nanoparticles highly sensitive to local changes in the dielectric environment, making them suitable for sensing applications.

Cylindrical nanoparticles (20×20 nm) are characterized by a red shift of 130 nm, from 375 to 505 nm, at an increase in the refractive index, from 1.0 to 1.7. A splitting of the plasmon resonance is also observed in this case, which is typical of anisotropic structures with longitudinal and transverse modes (see Fig. 6b).

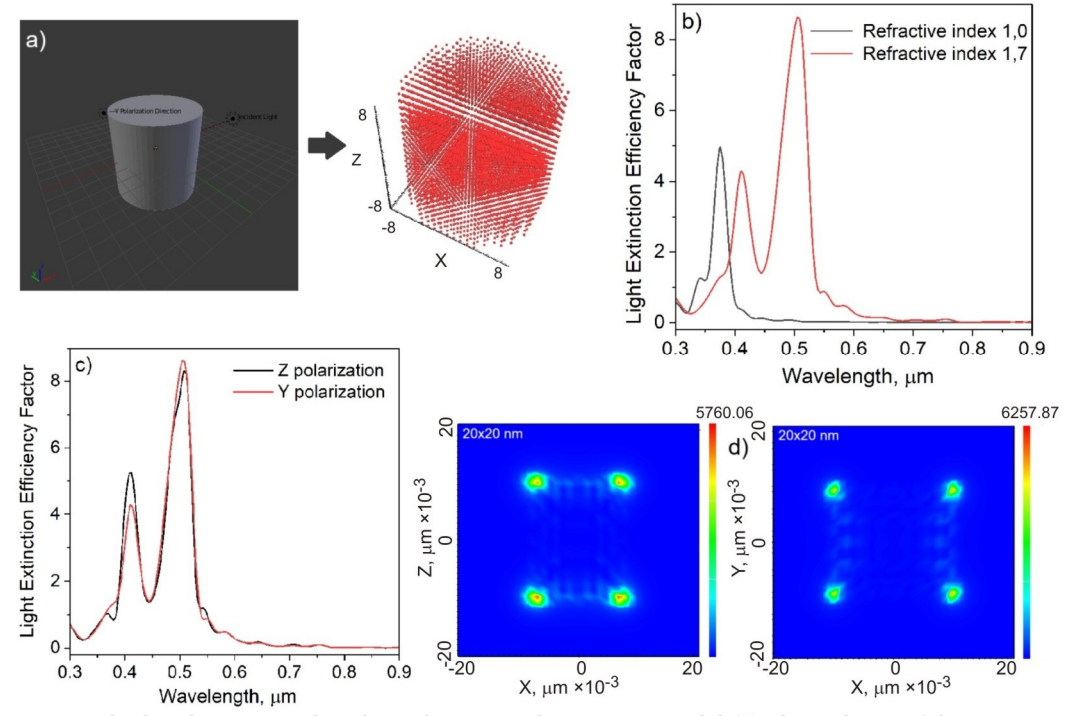


Fig. 6. Cylindrical nanoparticles: three-dimensional geometric model (a); dependence of the extinction coefficient on the wavelength for different refractive indices of the surrounding medium (b); dependence of the extinction coefficient on the wavelength for different directions of polarization (c); electromagnetic field distribution (d).

The effect of orientation is less pronounced in the extinction spectra of such nanoparticles with the same height and diameter due to the absence of significant geometric anisotropy (Fig. 6c). However, detailed modelling of the electric field distribution showed that the maximum intensity increased from 5.760 V/m in *Z*-polarization (the field was parallel to the cylinder axis) to 6.258 V/m in *Y*-polarization (the field was perpendicular to the axis) (see Fig. 6d). This relatively weak dependence is due to the cylinders under study having an aspect ratio close to unity. The orientation effect should be much stronger for more elongated cylindrical nanoparticles, similar to ellipsoids.

The behaviour of cylindrical nanoparticles differs qualitatively from that of ellipsoids and cubes when geometric parameters are altered. Their plasmonic properties are determined by the complex interaction of longitudinal and transverse modes, resulting in non-monotonic spectral characteristic dependencies on the aspect ratio.

There is not a monotonic shift of a single resonance for a series of cylinders with a constant diameter of 20 nm and lengths ranging from 20 to 80 nm, but rather a redistribution of intensity between two plasmon modes of different symmetry (see Fig. 7). A cylinder with an aspect ratio of 1:1 is characterized by two peaks. The first is at 410 nm. This is low intensity. The second is at 508 nm. This is high intensity. As the cylinder's height increases, its spectral structure changes. For an 80-nm-long cylinder (with an aspect ratio of 4:1), an inversion of the intensity ratio is observed. The intense peak is now localized at 393 nm, while the long-wave peak at \sim 500 nm is significantly weaker. This non-monotonic behavior reflects the complex interaction between longitudinal and transverse plasmon modes as the cylinder's aspect ratio is varied. This phenomenon occurs due to competition between the longitudinal mode, which involves oscillations of electrons along the cylinder's

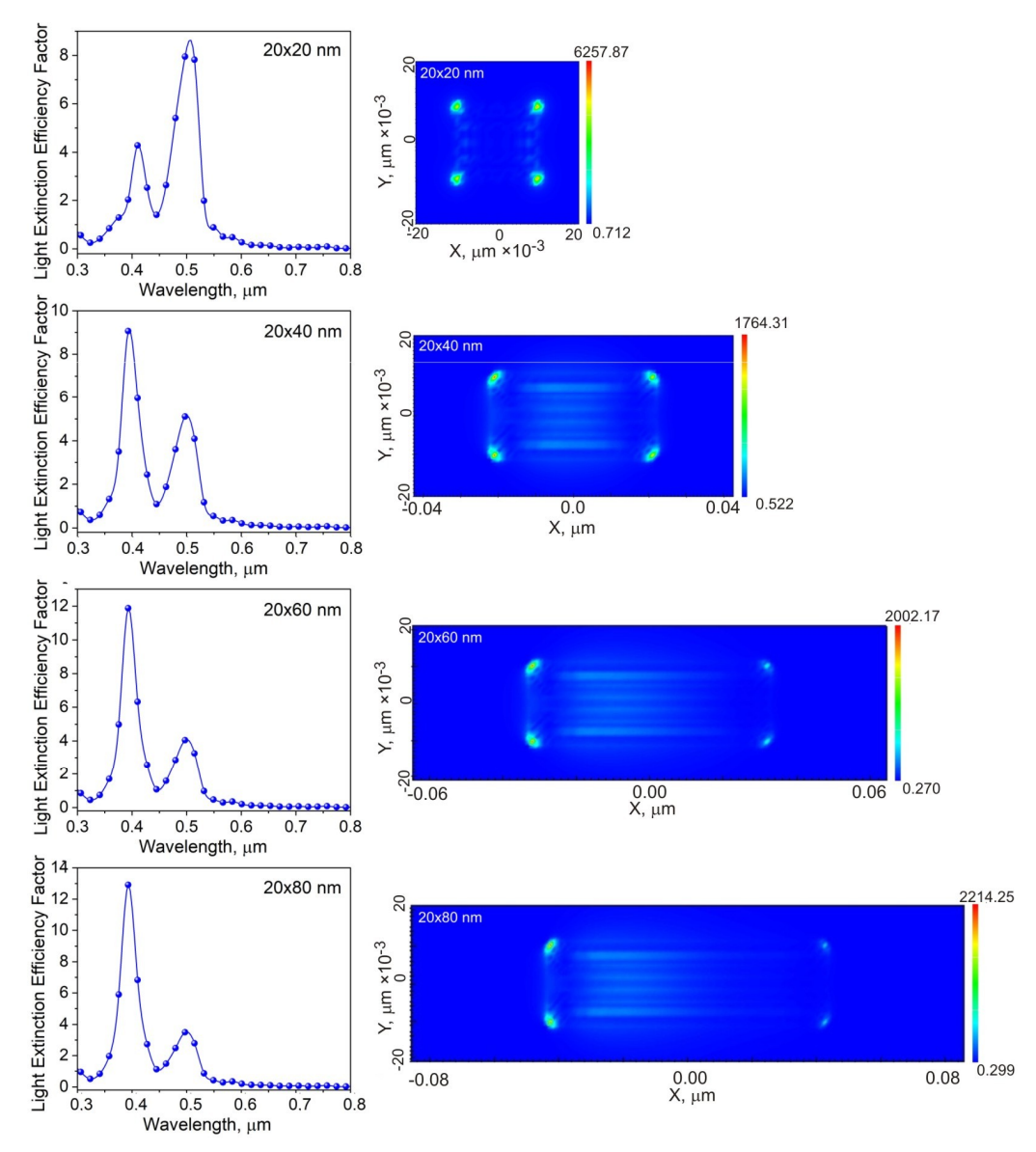


Fig. 7. Cylindrical nanoparticles: dependence of the extinction coefficient on the wavelength and electromagnetic field distribution for the different sizes of the nanoparticles.

axis, and the azimuthal modes, which involve oscillations around the cylinder's circumference [43]. With a short cylinder, azimuthal modes are dominant, but with elongation, the longitudinal mode increases because the depolarization factor decreases.

Significant changes in the electric field distribution also occur when the cylinder geometry is varied (see Fig. 7). For a 20 nm cylinder, symmetrical field localization is observed at both flat bases, where the curvature changes sharply from zero at the plane to large at the base edge. As the cylinder's height increases, this symmetry is broken, and the field becomes concentrated mainly on the illuminated base, on the side facing the electromagnetic wave's incidence, with exponential attenuation along the cylindrical surface. This transformation is evident in the shift from a standing-wave regime for a short cylinder to a travelling-wave regime with absorption for a long cylinder [44]. The strength of the electric field shows a non-monotonic relationship with the cylinder length, with a minimum at intermediate values. This minimum is reached when destructive interference between different plasmon modes is most pronounced. The field strength increases for both very short and very long cylinders due to the dominance of a single mode.

Sharp edges at the boundary of the base and lateral surface are a defining feature of cylinders, which are distinct from ellipsoids with their smooth, rounded ends. These edges are lines of curvature discontinuity. This leads to the electric field becoming more localized and specific edge modes becoming excited [45]. The complex spectral structure of cylindrical nanoparticles is determined by the interaction of edge modes with longitudinal and azimuthal modes. When polarized light propagates along the cylinder's axis, dipole modes

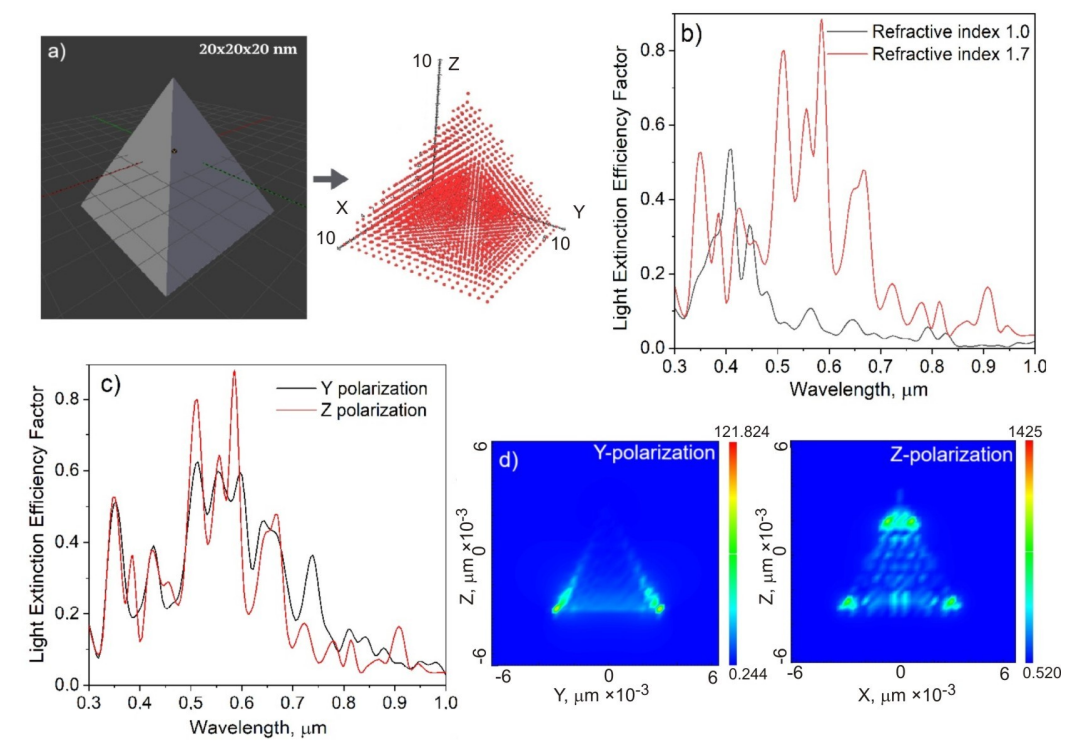


Fig. 8. Prismatic nanoparticles: three-dimensional geometric model (a); dependence of the extinction coefficient on the wavelength for different refractive indices of the surrounding medium (b); dependence of the extinction coefficient on the wavelength for different directions of polarization (c); distribution of the electromagnetic field (d).

are excited, as shown in the extinction spectra. Higher-order modes can be excited by unpolarized light or by complex illumination geometry, leading to even greater complexity in spectral characteristics.

Unlike the other nanoparticles studied above, prismatic nanoparticles exhibit a particularly complex transformation of their extinction spectra when the dielectric environment changes (see Fig. 8b). Two clearly defined peaks are observed in air at around 400 and 440 nm. In the organic matrix, a series of resonances appear in the 500–600 nm range with increased intensity. The high sensitivity of prismatic geometry to environmental parameters makes these structures ideal for use in sensors, where detecting changes in refractive index is key.

The change in polarization showed that, for Y-polarization, the electric field intensity reaches a maximum of 121.8. In contrast, in the case of Z-polarization of the prism of the same size, the electric field intensity reaches 1425.6 (Fig. 8d). The amplitude of the extinction spectra in the case of Z-polarization is also larger than in the case of Y-polarization (Fig. 8c). Therefore, all further studies were carried out specifically for the Z-polarization configuration.

Prismatic nanoparticles with a square base are the most morphologically complex class of structure that has been studied, and they demonstrate the most pronounced sensitivity of plasmonic characteristics to geometric parameters. A study of prismatic nanoparticles with a square base measuring 20×20 nm and a height ranging from 20 to 80 nm revealed a red shift in the dominant plasmon resonance (see Fig. 9). For a prism with a height of 20 nm, a series of multimodal resonances in the range of 500-600 nm is observed. The dominant resonance shifts to around 1000 nm as the height increases to 80 nm, entering the near-infrared region of the spectrum. This shift, which is about 400-500 nm in magnitude, significantly exceeds the corresponding values for ellipsoids and other geometries with a comparable change in aspect ratio. This makes prismatic geometry particularly well-suited to applications that require the precise tuning of plasmon resonance spectral positions over a wide wavelength range. A change in the multimodal structure of the spectra, with a redistribution of intensities between individual peaks, is observed simultaneously with the shift of the dominant resonance. Prisms with small heights exhibit a complex pattern with several peaks of comparable intensity. In contrast, prisms with large heights form a single dominant resonance accompanied by additional weak features.

The electric field is extremely localized at the sharp apex of the pyramid, which is the most striking feature of prismatic nanoparticles (Fig. 9). The apex is cone-shaped. This is where the maximum concentration of electron density occurs. The electric field strength at the top can reach values one to two orders of magnitude greater than the incident wave's amplitude. The presence of these "hot spots", which are characterized by their unique properties for enhancing light-matter interactions, is a result of the extremely high local tension. It is important to note that localization intensity increases with prism height because the apex becomes relatively sharper and the angle at the apex decreases. Among all the geometries studied, the electric field enhancement factor at the apex is greatest for the highest prisms, with a height of 80 nm.

Therefore, we conducted a systematic analysis of four morphologies, which enabled us to identify general patterns and physical mechanisms that govern the plasmonic behavior of metal nanoparticles.

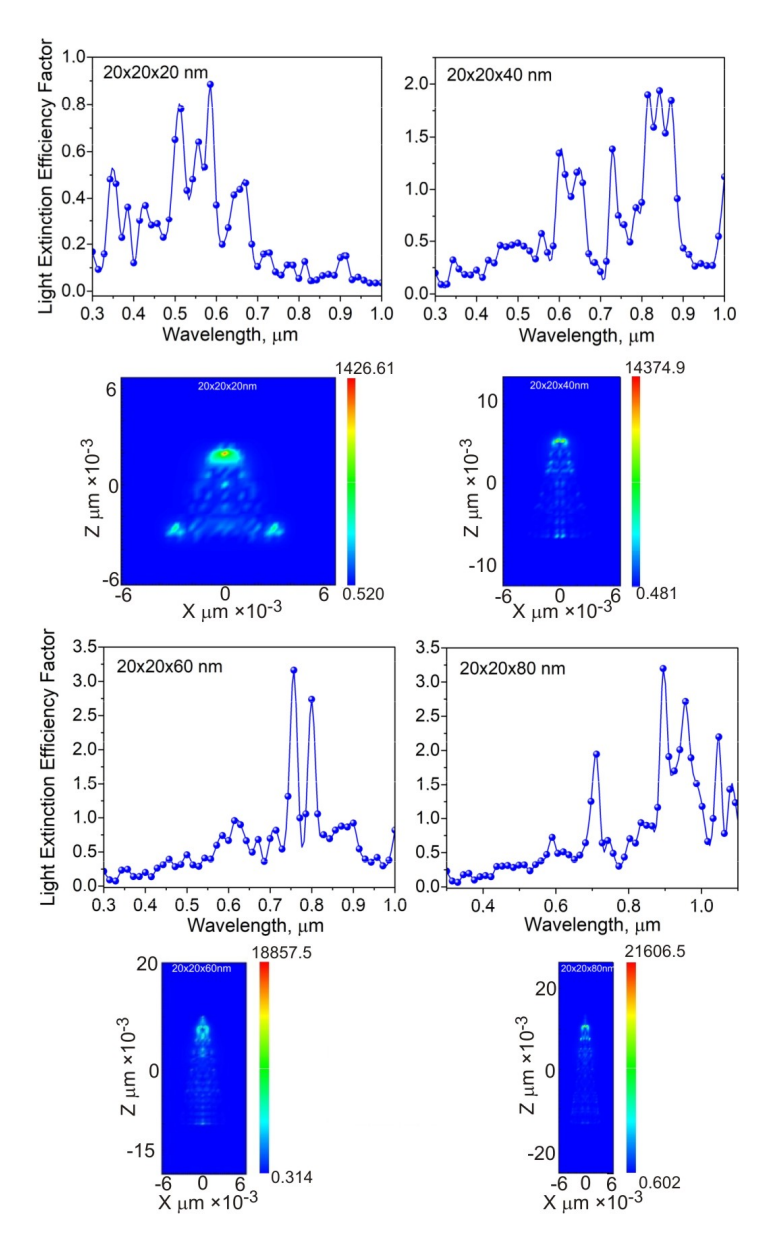


Fig. 9. Prismatic nanoparticles: dependence of the extinction coefficient on the wavelength and electromagnetic field distribution for different sizes of the nanoparticles.

It has been discovered that the optical response of anisotropic nanoparticles is critically dependent on their spatial orientation, opening new possibilities for the development of highly sensitive SERS sensor platforms and devices. Controlled amplification of a localized electromagnetic field enables high SERS enhancement factors in 'hot spots', enabling detection at the level of individual molecules. The orientation-dependent plasmonic properties of ellipsoidal, cubic, cylindrical, and prismatic nanoparticles can be exploited to create optical sensors that detect the spatial orientation of biomolecules and nanoobjects. In nanophotonics, anisotropic nanoparticles are used in optical devices that have controllable polarization selectivity and directional energy transport. Orientational control provides optical anisotropy in the near-infrared range. In light-emitting diodes (LEDs), including

organic light-emitting diodes (OLEDs), integrating plasmonic nanoparticles with specific geometries into the emission or transport layers increases device stability and radiation efficiency. This is achieved by accelerating radiative transitions and enhancing light emission via resonant coupling between localized plasmons and emitter excitons.

4. Conclusions

A systematic theoretical study was conducted using the discrete dipole method to establish the fundamental patterns of how morphology, geometric parameters, spatial orientation, and the dielectric environment influence the plasmonic characteristics of silver nanoparticles. Depending on the nanoparticle geometry, an increase in the medium's refractive index results in a red shift of the plasmon resonances by 130-190 nm. At the same time, an increase in the extinction efficiency coefficient is observed, indicating an increase in the interaction between plasmons and radiation in a medium with a higher dielectric permittivity. It was found that the optical response of anisotropic nanoparticles critically depends on their spatial orientation relative to the incident light's polarization. The most pronounced effect is observed for ellipsoidal nanoparticles with an aspect ratio of 2:1. Here, a change in orientation results in a 200 nm shift in the resonance spectrum and a threefold variation in the maximum electric field strength. The positions of plasmon resonances can be tuned over a wide spectral range (400-1000 nm) by varying geometric parameters. The spectral position of the resonance can be controlled most flexibly with ellipsoidal and prismatic nanoparticles, while cubic and cylindrical structures exhibit more complex multimodal behavior. The electric field is maximally localized in regions with the greatest local curvature, with amplification reaching factors of 10²–10³ at the sharp vertices of prismatic structures.

The results demonstrate the wide range of possibilities for morphological engineering of plasmonic properties to optimize light-matter interactions in nanostructured optoelectronic devices. The purposeful selection of the morphology, size, and orientation of metal nanoparticles enables resonant interaction with the operating spectral range of light-emitting or photovoltaic heterostructures. This increases their efficiency through mechanisms such as local field enhancement, light scattering, and modification of the radiative recombination rate.

Funding. The research presented in this paper was funded by the National Research Foundation of Ukraine (Grant No 0124U003833).

Conflict of interests. The authors have no conflicts to disclose.

References

- Krishchenko, I. M., Manoilov, É. G., Kravchenko, S. A., & Snopok, B. A. (2020). Resonant optical phenomena in heterogeneous plasmon nanostructures of noble metals: a review. *Theoretical and Experimental Chemistry*, 56(2), 67-110
- 2. Li, M., Cushing, S. K., & Wu, N. (2015). Plasmon-enhanced optical sensors: a review. Analyst, 140(2), 386-406.
- 3. Lv, S., Du, Y., Wu, F., Cai, Y., & Zhou, T. (2022). Review on LSPR assisted photocatalysis: effects of physical fields and opportunities in multifield decoupling. *Nanoscale Advances*, 4(12), 2608-2631.
- 4. Khani, S., & Rezaei, P. (2024). Optical sensors based on plasmonic nano-structures: A review. Heliyon, 10(24).
- 5. Khurana, K., & Jaggi, N. (2021). Localized surface plasmonic properties of Au and Ag nanoparticles for sensors: a review. *Plasmonics*, 16(4), 981-999.
- 6. Ashrafi, T. M. S., & Mohanty, G. (2025). Surface plasmon resonance sensors: a critical review of recent advances, market analysis, and future directions. *Plasmonics*, 1-21.
- 7. Wei, Y., Qin, M., Liu, Y., Jia, X., Zhou, J., & Wang, G. (2025, February). Easily prepared and high-performance AgNPs as SERS substrates for trace thiram detection. *In Journal of Physics: Conference Series*, 2961(1), 012006.
- 8. Zhang, Z., Liu, C., Dong, J., Zhu, A., An, C., Wang, D., Xue, M., Shijiing, Y.,& Zhang, Y. (2024). Self-Referenced Au Nanoparticles-Coated Glass Wafers for In Situ SERS Monitoring of Cell Secretion. *ACS sensors*, 9(8), 4154-4165.

- Araujo, P. F., Fernandes, R. S., Neto, O. F., Flauzino, E., de Souza, M. A., & Balaban, R. C. (2025). A new SERS substrate: Agnanoparticles immobilized on glass for rapid scale inhibitor determination

 Theoretical and experimental approach. Spectrochimica Acta Part A: Molecular and Biomolecular Spectroscopy, 341, 126442.
- Meškinis, Š., Peckus, D., Vasiliauskas, A., Čiegis, A., Gudaitis, R., Tamulevičius, T., . Yaremchuk, I. & Tamulevičius, S. (2017). Photovoltaic properties and ultrafast plasmon relaxation dynamics of diamond-like carbon nanocomposite films with embedded Ag nanoparticles. *Nanoscale Research Letters*, 12(1), 288.
- 11. Bulavinets, T., Yaremchuk, I., Bobitski, Y., & Barylyak, A. (2023). Synthesis and photocatalytic efficiency of plasmonic Ag/TiO₂: S nanosystems. *Applied Nanoscience*, *13*(7), 4693-4699.
- 12. Naseef, H. H., Al-Haddad, A., Albarazanchi, A. K., Jaafar, A., & Veres, M. (2025). Deep investigation of absorption enhancement through embedded plasmonic nanostructure into photovoltaics cells. *Plasmonics*, 20(7), 4671-4678.
- Hang, Y., Wang, A., & Wu, N. (2024). Plasmonic silver and gold nanoparticles: shape-and structure-modulated plasmonic functionality for point-of-caring sensing, bio-imaging and medical therapy. *Chemical Society Reviews*, 53(6), 2932-2971.
- Bulavinets, T., Kulpa-Greszta, M., Tomaszewska, A., Kus-Liśkiewicz, M., Bielatowicz, G., Yaremchuk, I., Barylyak, A., Bobitski, ya. & Pazik, R. (2020). Efficient NIR energy conversion of plasmonic silver nanostructures fabricated with the laser-assisted synthetic approach for endodontic applications. RSC Advances, 10(64), 38861-38872.
- Waketola, A. G., Tegegne, N. A., & Hone, F. G. (2025). Recent Progress in Silver and Gold Nanoparticle-Based Plasmonic Organic Solar Cells. *Plasmonics*, 20(7), 5521-5556.
- Kim, D. H., & Kim, T. W. (2016). Enhancement of the current efficiency of organic light-emitting devices due to the surface plasmonic resonance effect of dodecanethilol-functionalized Au nanoparticles. *Organic Electronics*, 34, 262-266.
- Georgiopoulou, Z., Verykios, A., Soultati, A., Chroneos, A., Hiskia, A., Aidinis, K., Skandamis, P.N., Gounadaki, A.S., Karatasios, I., Triantis, T.D., Argitis, P., Palilis, L.C. & Vasilopoulou, M. (2024). Plasmonic enhanced OLED efficiency upon silver-polyoxometalate core-shell nanoparticle integration into the hole injection/transport layer. Scientific Reports, 14(1), 28888.
- 18. Kang, K., Byeon, I., Kim, Y. G., Choi, J. R., & Kim, D. (2024). Nanostructures in Organic Light-Emitting Diodes: Principles and Recent Advances in the Light Extraction Strategy. *Laser & Photonics Reviews*, *18*(8), 2400547.
- 19. Liu, J., Meng, Z., & Zhou, J. (2024). High electric field enhancement induced by modal coupling for a plasmonic dimer array on a metallic Film. *Photonics*, 11(2), 183.
- Ammara, A., Abbas, G., Pepe, F. V., Afzaal, M., Qamar, M., & Ghuffar, A. (2023). The influence of substrate on the optical properties of gold nanoslits. *Journal of Imaging*, 9(12), 269.
- 21. Šubr, M., Petr, M., Kylián, O., Štěpánek, J., Veis, M., & Procházka, M. (2017). Anisotropic optical response of silver nanorod arrays: surface enhanced raman scattering polarization and angular dependences confronted with ellipsometric parameters. *Scientific Reports*, 7(1), 4293.
- Tiandho, Y., Septiani, N. L. W., Gumilar, G., Jonuarti, R., & Yuliarto, B. (2023). High-Performance Refractive Index-Based Sensor Using Ellipsoid Ag–Au Nanoparticles. *IEEE Sensors Journal*, 23(9), 9390-9401.
- 23. Perrakis, G., Kakavelakis, G., Kenanakis, G., Petridis, C., Stratakis, E., Kafesaki, M., & Kymakis, E. (2019). Efficient and environmental-friendly perovskite solar cells via embedding plasmonic nanoparticles: an optical simulation study on realistic device architectures. *Optics Express*, *27*(22), 31144-31163.
- 24. Mahmoud, M. A., Narayanan, R., & El-Sayed, M. A. (2013). Enhancing colloidal metallic nanocatalysis: sharp edges and corners for solid nanoparticles and cage effect for hollow ones. *Accounts of Chemical Research*, 46(8), 1795-1805.
- 25. Dabiri, M., Fazli, H., Salarinejad, N., & Movahed, S. K. (2021). Pd nanoparticles supported on cubic shaped ZIF-based materials and their catalytic activates in organic reactions. *Materials Research Bulletin*, 133, 111015.
- 26. Downing, C. A., & Weick, G. (2020). Plasmonic modes in cylindrical nanoparticles and dimers. *Proceedings of the Royal Society A*, 476(2244), 20200530.
- 27. Magarotto, M., Schenato, L., Franchin, G., Santagiustina, M., Galtarossa, A., & Capobianco, A. D. (2024). Cylindrical waveguides for microwave spoof surface plasmon polaritons. *IEEE Access*, 12, 23190-23199.
- 28. Minh Ngo, H., Drobnyh, E., Sukharev, M., Khuong Vo, Q., Zyss, J., & Ledoux-Rak, I. (2023). High yield synthesis and quadratic nonlinearities of gold nanoprisms in solution: The role of corner sharpness. *Israel Journal of Chemistry*, 63(12), e202200009.
- 29. Bulavinets, T., Rokhiv, V., Akopian, V., Bulavinets, B., Hladun, M., & Yaremchuk, I. (2025). Impact of shape on plasmon resonance in single silver nanoparticles: theoretical study. *Molecular Crystals and Liquid Crystals*, 1-12.
- Yan, Z., Taylor, M. G., Mascareno, A., & Mpourmpakis, G. (2018). Size-, shape-, and composition-dependent model for metal nanoparticle stability prediction. *Nano Letters*, 18(4), 2696-2704.
- 31. Dorodnyy, A., Smajic, J., & Leuthold, J. (2023). Mie scattering for photonic devices. *Laser & Photonics Reviews*, 17(9), 2300055.
- 32. Teixeira, F. L., Sarris, C., Zhang, Y., Na, D. Y., Berenger, J. P., Su, Y., Okoniewski M., Chew W.C., Backman V., Simpson, J. J. (2023). Finite-difference time-domain methods. *Nature Reviews Methods Primers*, 3(1), 75.

- 33. Ogáyar, M. P., López-Méndez, R., Figueruelo-Campanero, I., Muñoz-Ortiz, T., Wilhelm, C., Jaque, D., Espinosa A., Serrano, A. (2024). Finite element modeling of plasmonic resonances in photothermal gold nanoparticles embedded in cells. *Nanoscale Advances*, 6(18), 4635-4646.
- $34. \ \ Chaumet, P. C. \ (2022). \ The \ discrete \ dipole \ approximation: A \ review. \ \textit{Mathematics}, 10 (17), 3049.$
- 35. Arslanyürek, Ş., & Dinleyici, M. S. (2025). Functional manipulation of nonspherical nanoparticles with cascaded reconfigurable modules. *Optics Communications*, 132097.
- Sørensen, L. K., Gerasimov, V. S., Karpov, S. V., & Ågren, H. (2024). Development of discrete interaction models for ultrafine nanoparticle plasmonics. *Physical Chemistry Chemical Physics*, 26(37), 24209-24245.
- 37. Palik, E. D. (Ed.). (1998). Handbook of optical constants of solids (Vol. 3). Academic press.
- 38. Draine, B. T., & Flatau, P. J. User Guide for the Discrete Dipole Approximation Code DDSCAT 7.1 (2010). *Available from:* http. arXiv. org/abs/1202.3424.
- 39. Yurkin, M. A., & Hoekstra, A. G. (2007). The discrete dipole approximation: an overview and recent developments. *Journal of Quantitative Spectroscopy and Radiative Transfer*, 106(1-3), 558-589.
- 40. Zayats, A. V., Smolyaninov, I. I., & Maradudin, A. A. (2005). Nano-optics of surface plasmon polaritons. *Physics reports*, 408(3-4), 131-314.
- Collins, S. M., Ringe, E., Duchamp, M., Saghi, Z., Dunin-Borkowski, R. E., & Midgley, P. A. (2015). Eigenmode tomography
 of surface charge oscillations of plasmonic nanoparticles by electron energy loss spectroscopy. ACS photonics, 2(11),
 1628-1635.
- 42. Grigorchuk, N. I. (2012). Radiative damping of surface plasmon resonance in spheroidal metallic nanoparticle embedded in a dielectric medium. *Journal of the Optical Society of America B*, 29(12), 3404-3411.
- 43. Halas, N. J., Lal, S., Chang, W. S., Link, S., & Nordlander, P. (2011). Plasmons in strongly coupled metallic nanostructures. *Chemical Reviews*, 111(6), 3913-3961.
- 44. Sun, S., Chen, H. T., Zheng, W. J., & Guo, G. Y. (2013). Dispersion relation, propagation length and mode conversion of surface plasmon polaritons in silver double-nanowire systems. *Optics Express*, 21(12), 14591-14605.
- 45. Yu, H., Peng, Y., Yang, Y., & Li, Z. Y. (2019). Plasmon-enhanced light-matter interactions and applications. *npj Computational Materials*, 5(1), 45.

Bulavinets, T., Grokhotov, V., Helzhynskyy, I., Bulavinets, B., Stakhira, P., Yaremchuk, I. (2026). Morphological Engineering of Plasmonic Nanostructures: Simulation of Optical Response for Nanoparticles with Basic Geometries. *Ukrainian Journal of Physical Optics*, *27*(1), 01054 – 01069. doi: 10.3116/16091833/Ukr.J.Phys.Opt.2026.01054

Анотація. Системне чисельне дослідження плазмонних властивостей металевих наночастинок базових геометрій, а саме еліпсоїдальної, кубічної, циліндричної та призматичної проведено методом дискретної дипольної апроксимації. Встановлено, що спектральне положення локалізованих поверхневих плазмонних резонансів має виражену анізотропію з можливістю широкосмугового налаштування (від видимого до ближнього інфрачервоного діапазону) шляхом варіювання морфологічних параметрів та орієнтації частинок відносно напрямку поширення електромагнітної хвилі. Аналіз просторового розподілу ближнього поля виявив закономірності локалізації електромагнітного поля в зонах з максимальною кривизною поверхні, що корелює з появою областей значного підсилення. Показано, що резонансна поведінка анізотропних наноструктур визначається сукупністю взаємопов'язаних факторів: тензором коефіцієнтів деполяризації, що визначає спектральне положення дипольних мод; виникненням мультипольних резонансів вищих порядків для геометрій зі складною симетрією; а також розмірно-залежним радіаційним загасанням. Отримані результати формують фундаментальну базу для раціонального дизайну плазмонних наночастинок із заданими оптичними характеристиками для застосувань в оптоелектроніці, сенсориці, та спектроскопії.

Ключові слова: локалізований поверхневий плазмонний резонанс, наночастинки, метод дискретної дипольної апроксимації, локалізація електричного поля